Research paper

New technique to quantify chaotic dynamics based on differences between semi-implicit integration schemes

Denis N. Butusov [a,*], Dmitriy O. Pesterev [b], Aleksandra V. Tutueva [b,*], Dmitry I. Kaplun [c], Erivelton G. Nepomuceno [d]

[a] Youth Research Institute, Saint-Petersburg Electrotechnical University "LETI", 5, Professora Popova st., Saint Petersburg 197376, Russia
[b] Department of Computer-Aided Design, Saint Petersburg Electrotechnical University "LETI", 5, Professora Popova st., Saint Petersburg 197376, Russia
[c] Department of Automation and Control Processes, Saint Petersburg Electrotechnical University "LETI", 5, Professora Popova st., Saint Petersburg 197376, Russia
[d] Control and Modelling Group (GCOM), Department of Electrical Engineering, Federal University of São João del-Rei, São João del-Rei, MG 36307-352, Brazil

A R T I C L E   I N F O

A B S T R A C T

Many novel chaotic systems have recently been identified and numerically studied. Parametric chaotic sets are a valuable tool for determining and classifying oscillation regimes observed in nonlinear systems. Thus, efficient algorithms for the construction of parametric chaotic sets are of interest. This paper discusses the performance of algorithms used for plotting parametric chaotic sets, considering the chaotic Rossler, Newton-Leipnik and Marioka-Shimizu systems as examples. In this study, we compared four different approaches: calculation of largest Lyapunov exponents, statistical analysis of bifurcation diagrams, recurrence plots estimation and introduced the new analysis method based on differences between a couple of numerical models obtained by semi-implicit methods. The proposed technique allows one to distinguish the chaotic and periodic motion in nonlinear systems and does not require any additional procedures such as solutions normalization or the choice of initial divergence value which is certainly its advantage. We evaluated the performance of the algorithms with the two-stage approach. At the first stage, the required simulation time was estimated using the perceptual hash calculation. At the second stage, we examined the performance of the algorithms for plotting parametric chaotic sets with various resolutions. We explicitly demonstrated that the proposed algorithm has the best performance among all considered methods. Its implementation in the simulation and analysis software can speed up the calculations when obtaining high-resolution multi-parametric chaotic sets for complex nonlinear systems.

1. Introduction

Over the past decades, the number of publications considering new chaotic systems and their applications has increased significantly [1–6]. In that regard, J.C. Sprott in [7] proposed a standard that establishes the requirements for research

---

* Corresponding authors.
E-mail addresses: dnbutusov@etu.ru (D.N. Butusov), dopesterev@etu.ru (D.O. Pesterev), avtutueva@etu.ru (A.V. Tutueva), dikaplun@etu.ru (D.I. Kaplun), nepomuceno@ufsj.edu.br (E.G. Nepomuceno).

published in nonlinear dynamics. The considered criteria for mathematical models of new chaotic systems include three properties: simplicity, physical motivation, and novelty. Moreover, Sprott claimed that an important part of the study is a comprehensive investigation of the entire parameter space to identify all possible types of dynamic behaviors. We should also note that it is important to investigate phenomena observed in new chaotic systems including hidden attractors [8], multi-parametric bifurcations [9], chimera states [10], etc. However, the reliability of the results of parametric analysis significantly depends on the chosen initial conditions. Bifurcation diagrams may look very different depending on how the initial conditions are chosen [7]. Therefore, a separate study of the parametric sets is also a critical part of the analysis of the new chaotic system.

To study the parameter spaces many quantitative and qualitative metrics have been proposed [11]. The application of quantitative metrics reduces the impact of expert assessments on the results. As quantitative metrics of the system behavior the Largest Lyapunov exponent [12], the Kolmogorov-Sinai [13] and Tsallis entropy [14], various system space dimensions [15,16] and other measures [17–19] can be applied. A thorough analysis of the chaotic system involves multiple simulations with various parameters and initial conditions. The obtained values are usually plotted as parametric chaotic sets [20]. It is still an open question of how one should choose a time interval for calculating certain quantitative metrics to obtain reliable results with desirable precision [21]. In some cases, it is time-consuming to construct a two-parametric chaotic set using metrics based on highly complex algorithms while the time complexity of constructing the parametric chaotic set itself is $O(N^2)$. Moreover, it is of great importance to minimize the simulation time, since in the long-term simulations numerical methods can significantly influence the system dynamics and change its properties [22,23]. In addition, many algorithms for quantitative metrics calculation include parameters that should be thoroughly evaluated to obtain reliable parametric chaotic sets. Thus, it is of interest to develop the dynamical analysis algorithms free of any auxiliary analytical procedures such as normalization or the choice of an initial divergence.

The novelty of this study consists of two main advances. First, we propose a technique for experimental evaluation of the minimum simulation time required for the convergence of common quantitative metrics of chaos. Moreover, we considered new metrics for dynamical analysis of chaotic systems. These metrics are based on a relative integration error (RIE) of a pair of numerical models obtained by different semi-implicit methods, known as CD-methods [24,25]. It is expected, that this value will correlate with the small changes in chaotic system oscillations. We investigated four algorithms for parametric analysis of system dynamics and compare their time complexity and the computation costs for constructing two-parametric chaotic sets. We considered the kernel density estimation as quantitative metrics of bifurcation diagrams [26], the largest Lyapunov exponent value [27–29], the inverse value of the longest diagonal line length of a recurrence plot [30,31] and introduced the new metrics based on a divergence between the pair of semi-implicit methods.

The rest of the paper is organized as follows. In Section 2, we present the RIE algorithm and illustrate the possibility to distinguish chaotic and periodic behavior with it. Then we propose the technique for choosing the minimal simulation time for the investigation of chaotic systems by calculating quantitative metrics. In Section 3 we introduce three sample chaotic systems. In Section 4, we present the results of the convergence investigation for four considered algorithms and compare their performance. Finally, some conclusions are given in Section 5.

2. Novel quantitative metrics for chaotic systems analysis

In this section, we mainly focus on the new quantitative technique for studying chaotic systems. Then we present an approach that allows to compare the proposed method with several algorithms from various areas such as signal processing, nonlinear dynamics, statistics, and computational mathematics. We considered the kernel density estimation (KDE), the largest Lyapunov exponent value (LLE), the inverse value of the longest diagonal line length of a recurrence plot (LDL). Algorithms for calculating these metrics are presented in Appendix B–Appendix D, respectively. We use the notations listed in Appendix A.

2.1. The relative integration error

The main concept of the RIE analysis basically follows the idea of the LLE calculation. It supposes the estimation of the average rate of exponential divergence between two trajectories starting from the same point and obtained by two different semi-implicit numerical integration methods.

Let us write numerical integration methods F_h and G_h in terms of the increment function Φ_h and its adjoint counterpart Φ_h^*:

$$\mathbf{x} = \mathbf{x} + h\Phi_h(\mathbf{x}, t),$$
$$\mathbf{y} = \mathbf{y} + h\Phi_h^*(\mathbf{y}, t).$$

From the properties of the *adjoint* methods it follows that after the first integration step the true trajectory of the system $\bar{\mathbf{x}}(t)$ will be approximated by $\mathbf{x}$ and $\mathbf{y}$ with following errors:

$$\bar{\mathbf{x}}(t_1) - \mathbf{x}_1 = h^p C(\mathbf{x}_0, t) + O(h^{p+1}),$$
$$\bar{\mathbf{x}}(t_1) - \mathbf{y}_1 = -h^p C(\mathbf{x}_0, t) + O(h^{p+1}),$$

where p is the order of the method's local truncation error and C is the function common for both methods.

The next integration step yields:

$$\bar{\mathbf{x}}(t_2) - \mathbf{x}_2 = h^p C\big(\bar{\mathbf{x}}(t_1) - h^p C(\mathbf{x}_0, t) + O(h^{p+1})\big) + (O)(h^{p+1}).$$

$$\bar{\mathbf{x}}(t_2) - \mathbf{y}_2 = -h^p C\big(\bar{\mathbf{x}}(t_1) + h^p C(\mathbf{x}_0, t) + O(h^{p+1})\big) + (O)(h^{p+1}).$$

Denoting $h^p C(\mathbf{x}, t) = \varepsilon_h(\mathbf{x}, t)$ we express the difference $\mathbf{x}_1 + \mathbf{y}_1$ as

$$\Delta_1 = \Phi_h(\mathbf{x}_0 + \varepsilon_h(\mathbf{x_0}, t_0), t_0) - \Phi_h^*(\mathbf{x}_0 - \varepsilon_h(\mathbf{x_0}, t_0), t_0),$$

which relates to the real trajectory $\mathcal{F}_h(\mathbf{x}, t)$ as

$$\Delta_1 = \mathcal{F}_h(\mathbf{x}_0 + \varepsilon_h(\mathbf{x}_0, t_0), t_0) - \mathcal{F}_h(\mathbf{x}_0 - \varepsilon_h(\mathbf{x}_0, t_0), t_0) + O(h^{p+1}).$$

This resembles the LLE calculation algorithm up to normalization using $||\varepsilon_h||$. Finally, the RIE metrics yields a value

$$\omega = \frac{1}{T_s} \ln \left\| \sum_{i=0}^{T_s/T_n - 1} \mathcal{F}_h^{T_n/h}(\mathbf{x}_i + \varepsilon_h(\mathbf{x}_i, t_i), t_i) - \mathcal{F}_h^{T_n/h}(\mathbf{x}_i - \varepsilon_h(\mathbf{x}_i, t_i), t_i) + O(h^{p+1}) \right\|,$$

which characterizes the rate of trajectory divergence due to a small perturbation $\varepsilon_h(\mathbf{x}_i, t_i)$.

The value ω relates to the LLE value in the following way:

$$\omega \approx \lambda + \frac{1}{T_s} \ln ||\varepsilon_h(\mathbf{x}_0, t_0)||.$$

One of the key features of LLE analysis is the ability to identify the type of behavior for the investigated system. Generally, if for certain parameters the LLE is positive, then the system presents chaotic dynamics. In the case of RIE, a bit more complicated rule should be selected:

$$\theta = \frac{1}{T_s} \ln ||\varepsilon_h(\mathbf{x}_0, t_0)||.$$

Regions where $\omega > \theta$ should be classified as chaotic. Estimation of $\varepsilon_h(\mathbf{x}_0, t_0)$ is performed once after the first integration step. Runge's rule is one of the possible approaches here. The implementation of the proposed threshold is illustrated in Fig. 1 together with traditional LLE calculation. We plotted the bifurcation diagram of the Rossler system in the middle to clarify the comparison of these two metrics. One can see, that the proposed threshold selection method is valid and the RIE algorithm allows one to distinguish chaotic and non-chaotic behavior in a bit more explicit way than LLE analysis. Moreover, the threshold formula includes integration stepsize, which reveals the possibility to efficiently implement RIE in simulations with adaptive stepsize and reduces the influence of the stepsize to the metrics calculation.

The two numerical integration methods chosen for RIE calculation should possess equal stability and geometrical properties. To satisfy this condition, we highly recommend using a pair of semi-implicit CD-methods with different *commutation matrix* [32]. The commutation matrix comprises of zeros and ones and defines integration variables actuation moments, n or $n + 1$, respectively. For an implicit algorithm the commutation matrix consists of ones, the explicit algorithm has the commutation matrix filled with zeros. In a semi-implicit method description, we use the brackets denoting an implicit state variable calculation in diagonals. Let us consider two adjoint semi-implicit methods with a complementary commutation matrix

$$\begin{pmatrix} 0 & 0 & 0 \\ 1 & 0 & 0 \\ 1 & 1 & 0 \end{pmatrix} \text{ and } \begin{pmatrix} [1] & 1 & 1 \\ 0 & [1] & 1 \\ 0 & 0 & [1] \end{pmatrix}. \tag{1}$$

Taking the integration step as $h/2$, the composition of two methods with commutation matrix (1) gives a symmetric *self-adjoint* CD-method of accuracy order two. It should be noted that due to the algebraic properties of the geometrical integrators, the pair of CD-methods with different commutation matrices are very close in numerical stability and geometric properties to each other. Moreover, they allow preserving geometrical properties of the solution during the conservative systems simulation. Thus, the hypothesis is that the relative error obtained for two models correlates mainly with the speed of phase space trajectories divergence as it stands for the traditional LLE calculation. Algorithm 1 represents a sequence of steps for calculating the RIE metrics.

It should be noted that in comparison to other dynamical analysis methods RIE does not require the introduction of extra parameters such as initial divergence or normalization time. The main adjustable parameter here is the order of calculation in semi-implicit numerical integration methods. This feature simplifies the computations and, therefore, decreases the time needed for obtaining high-resolution parametric chaotic sets. However, it is of interest to compare the possibility of performing RIE metrics with various integration operators. In Fig. 2 we compared the parametric chaotic sets for the Rossler system obtained by the RIE technique for different ODE solvers. First, we tested the case of two explicit midpoint methods with the different order of calculations in the right-hand-side of the system. It is known, that due to the high sensitivity of chaotic systems, trajectories of such discrete models should diverge. Two other cases were explicit Runge–Kutta 2 method plus explicit midpoint and explicit midpoint plus implicit midpoint. The results of the RIE analysis of the Rossler system obtained by various combinations of numerical methods are shown in Fig. 2. One can see, that the RIE metrics based on a pair of semi-implicit methods provides the best results among the investigated versions.
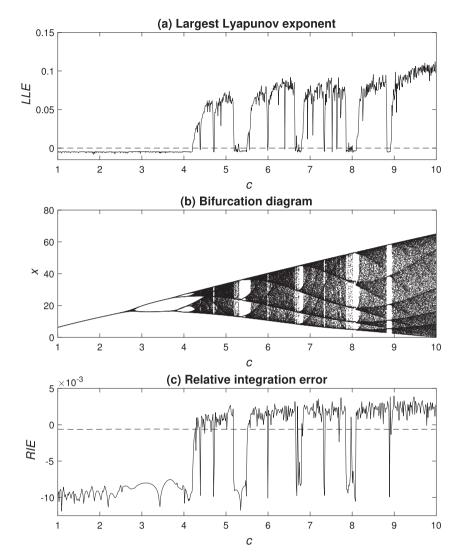
Fig. 1. The analysis of Rossler system behavior by LLE (a) and RIE (c) metrics. The threshold for RIE is $\theta = 0.0005$ and the integration stepsize is $T_s = 0.01$ s. Parameter c was varied in range from 1 to 10.

Algorithm 1: RIE calculation algorithm.

---

input   : A discrete operators of the system evolution F_h and G_h, an integration step h, an initial condition $\mathbf{x}_0$, an initial
             time t_0 a simulation time T_s

output: An average logarithmic local truncation error ω

$t = t_0$;

$\mathbf{x} = \mathbf{x}_0$;

$\mathbf{y} = \mathbf{x}_0$;

for $i = 1 : T_s/h$ **do**

   | *Compute next iteration*;

   | $\mathbf{x} = F_h(\mathbf{x}, t)$;

   | $\mathbf{y} = G_h(\mathbf{y}, t)$;

   | $t = t + h$;

end

Compute average logarithmic error;

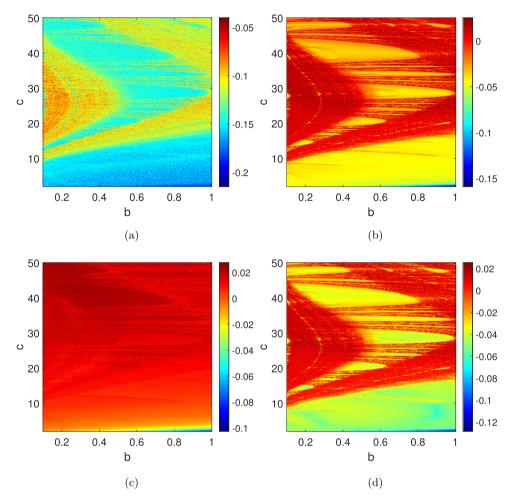$\omega = \ln ||\mathbf{y} - \mathbf{x}||/T_s$;

Fig. 2. The parametric chaotic sets for the Rossler system obtained by RIE technique for (a) two explicit midpoints methods with different order of calculations (b) explicit midpoint and second-order Runge–Kutta method (c) explicit and implicit midpoint methods (d) two semi-implicit CD-methods.

2.2. The technique for quantitative metrics comparison

A number of studies, e.g. [33], deal with the convergence of quantitative chaos metrics. The obtained values are influenced simultaneously by many factors such as simulation time, data type, accuracy order of the integration method and others. In this section, we consider a generalized method for choosing the minimal simulation time when calculating any quantitative metrics of the system behavior. Our technique consists of the following steps:

1. The sufficiently long simulation time T_{max} for the certain quantitative metrics is defined assuming that for the investigated chaotic system in simulation interval T_{max} the considered approach makes possible the construction of a parametric chaotic set with the desired precision.
2. For the time T_{max}, we construct the parametric chaotic set in $M \times M$ pixels resolution, which we will take as a reference.
3. We iterate the simulation time down with the step of Δt seconds performing the dynamical analysis on each step and comparing the output array of data with the reference one.
4. The simulation time for the determination of quantitative metrics is chosen by the criterion of similarity of methods map to the reference map. The minimal level of similarity is set to 95%.

The approach to the comparison of parametric chaotic sets is based on the calculation of their perceptual hash functions which is a common tool in image processing [34]. For the matrix representing the values of the quantitative metrics for the chaotic set, we calculated the average value and used it as a threshold. For values above the average, we put one, otherwise, we put zero. Thus, we obtained the hash of the parametric space set, which can be compared with the hash of the reference set through the calculation of the Hamming distance (see Fig. 3 as examples). For simplification, we normalized the obtained values to resolution map squared. Thus, we obtained a dimensionless value that allows the comparison of the different metrics to each other.
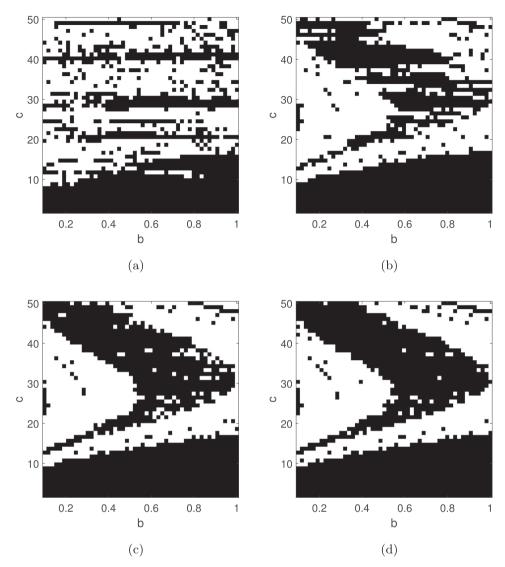
Fig. 3. The hash for parametric chaotic set obtained by the LLE method over simulation time (a) $t = 50$ sec (b) $t = 200$ sec (c) $t = 500$ sec (d) $t = 800$ s (reference) for the Rossler system.

We used this technique to evaluate all of the considered algorithms and then compared the time costs of the two-parametric chaotic sets construction.

3. Chaotic systems under investigation

Processes which possess the phenomenon of chaotic motion can be described by difference equations [35–37], ordinary differential equations (ODE) [38–40], partial differential equations [41,42], differential-algebraic equations, etc. Furthermore, time series often are the only available information about the real nonlinear phenomena. Multiple dynamical analysis methods such as recurrence plots can be used directly for time series investigation. For other quantitative metrics, e.g. LLE, calculation algorithms initially were formulated for the ODE system and can be applied to various types of differential equations or time series only using more complex techniques [29,43].

In our study, to compare quantitative metrics algorithms, we considered three chaotic systems including the well-known Rossler model as well as two systems with the minimal required dimension of the parameters space.
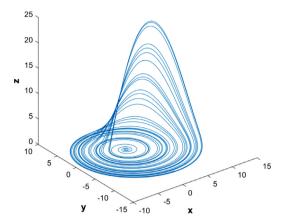
Fig. 4. The phase space of the Rossler system with trajectories started from $(0.1, 0, -0.11)$ with parameters $(0.2, 0.2, 5.7)$.
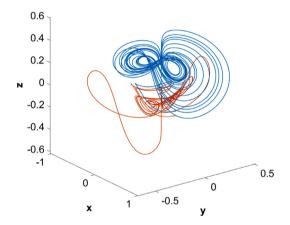

Fig. 5. The phase space of the Newton-Leipnik system with trajectories started from $(0.349, 0, -0.18)$ and $(0.349, 0, -0.16)$.

3.1. The Rossler chaotic system

One of the conventional models in deterministic chaos research is the Rossler system [39]. This system is described by the following ODEs

$$\begin{cases} \dot{x} = -y - z \\ \dot{y} = x + ay \\ \dot{z} = b + z(x - c) \end{cases} \tag{2}$$

where a, b, c are parameters. The phase space of system (2) with $a = 0.2$, $b = 0.2$ and $c = 5.7$ is shown in Fig. 4

In our experiments we varied parameters b and c within intervals [0.1; 1] and [2; 50], respectively.

3.2. The Newton-Leipnik system

The Newton-Leipnik system was first proposed in [44], thoroughly investigated in [45] and can be described by the following ODEs

$$\begin{cases} \dot{x} = -\alpha x + y + 10yz \\ \dot{y} = -x - 0.4y + 5xz. \\ \dot{z} = \beta z - 5xy \end{cases} \tag{3}$$

The system (3) exhibits chaotic behavior for values $\alpha = 0.4$, $\beta = 0.175$ and possesses the phase space with two attractors as is shown in Fig. 5.

In our experiments we varied parameters α and β within intervals [0.25; 1] and [0.02; 0.2], respectively.
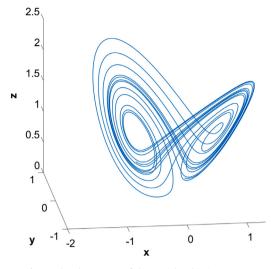
Fig. 6. The phase space of the Marioka-Shimizu system.

Table 1
Input values of the investigated algorithms.

Metric	Rossler	Newton-Leipnik	Marioka-Shimizu
LLE	$\varepsilon = 10^{-8}$, $T_n = 0.5\ s$	$\varepsilon = 10^{-8}$, $T_n = 0.5\ s$	$\varepsilon = 10^{-8}$, $T_n = 0.5\ s$
KDE	$h_s = 0.1\ s$, $k_s = 10$	$h_s = 0.005\ s$, $k_s = 10$	$h_s = 0.005\ s$, $k_s = 10$
LDL	$T_{dec} = 0.1\ s$, $\epsilon = 0.005$	$T_{dec} = 0.1\ s$, $\epsilon = 0.05$	$T_{dec} = 0.1\ s$, $\epsilon = 0.005$

3.3. The Marioka-Shimizu system

The third studied system was proposed by T. Shimizu and N. Morioka in [46]. It consists of three ODEs

$$\begin{cases} \dot{x} = y \\ \dot{y} = x - xz - \alpha y \\ \dot{z} = x^2 - \beta z \end{cases} \tag{4}$$

where $\alpha = 0.75$, $\beta = 0.45$ are common parameters for the simulation. This system exhibits similar behavior as the Lorenz model [46]. The phase space of the system is presented in Fig. 6.

To construct parametric chaotic sets we varied the parameters α and β in the ranges [0.2; 1] and [0.1; 0.5], respectively.

4. Experimental results

Let us apply the described analysis techniques to the sample chaotic systems. The experimental part of the study consisted of two steps. First, we evaluated the time of convergence for each of the studied metrics. Then, we considered the computational complexity of the algorithms and evaluated the time costs of constructing two-parametric chaotic sets. We chose the CD semi-implicit method as ODEs solver with the stepsize $h = 0.01\ s$. The initial conditions for all studied systems were $(0.1; -0.2; 0.1)$. Other parameters for calculating studied quantitative metrics are presented in Table 1.

All experiments were performed by NI LabVIEW 2018 64-bit simulation software on the desktop-class PC (Intel Core i5-4460, 8GB RAM) with Windows 10 operating system. We used the *double* floating-point data type [47] for calculations.

4.1. The convergence analysis

Let us plot the reference maps and their hashes on time interval $T_{\max} = 800\ s$. We assume that for all systems in this interval, any of the considered approaches is able to produce the parametric chaotic set with desirable precision. We iterate the simulation time down by the step $\Delta t = 50\ s$. The final time is 600 s. Figs. 7–9 represent the dependence between the normalized Hamming distance and the simulation time needed to construct relevant parametric chaotic sets of both investigated system for the considered algorithms.

One can see, that LDL method is the most time-consuming algorithm for the Newton-Leipnik system. However, it demonstrates better convergence than LLE and KDE metrics in cases of the Rossler and Marioka-Shimizu systems. The proposed RIE method demonstrates the best convergence for all considered systems. Moreover, one can notice that the rate of convergence
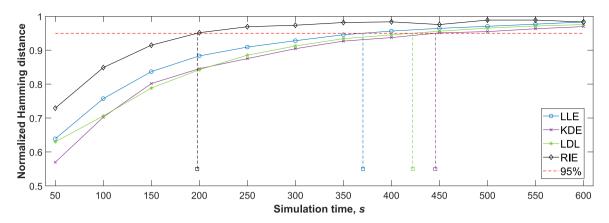
Fig. 7. The dependence between the normalized Hamming distance and the simulation time for the compared algorithms for the Rossler system.
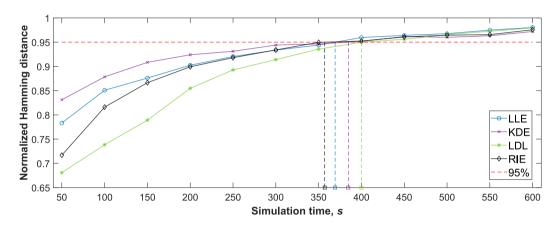

Fig. 8. The dependence between the normalized Hamming distance and simulation time for the compared algorithms for the Newton-Leipnik system.
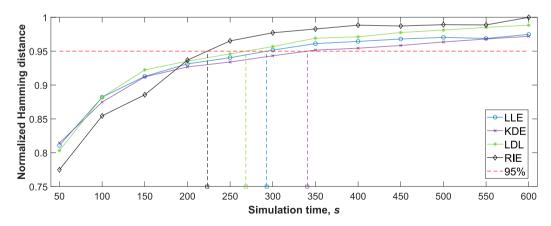

Fig. 9. The dependence between the normalized Hamming distance and the simulation time for the compared algorithms for the Marioka-Shimizu system.

of RIE is higher than that of the LLE algorithm. This can be illustrated well by the example of the Rossler system (Fig. 7). Table 2 represents estimated time values for each analysis method.

4.2. The performance comparison

The goal of this section is to experimentally investigate the performance of various algorithms for parametric chaotic set construction. Thus, the computational complexity of considered algorithms is the main target. This estimation highly depends on algorithm properties for calculating quantitative metrics. For example, the time costs on calculating, LDL

Table 2

Simulation time for investigated systems.

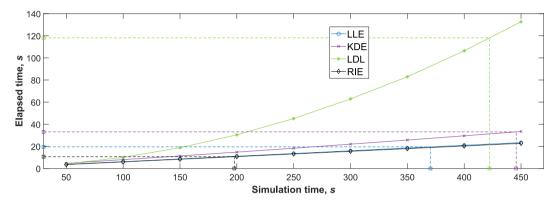| Metric	Time, *s*		
	Rossler	Newton–Leipnik	Marioka–Shimizu
LLE	362	370	293
KDE	448	385	340
LDL	438	400	267
RIE	200	355	223

Fig. 10. The dependence between time costs and the simulation time for the compared algorithms. The Rossler system.
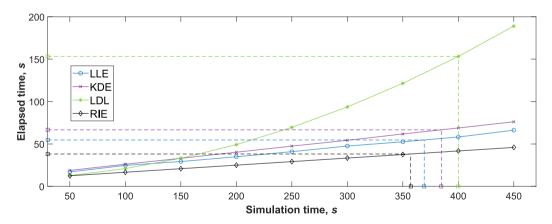

Fig. 11. The dependence between time costs and the simulation time for the compared algorithms. The Newton-Leipnik system.
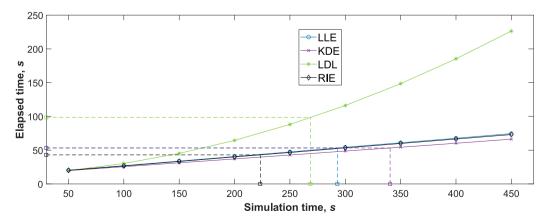

Fig. 12. The dependence between time costs and the simulation time for the compared algorithms. The Marioka-Shimizu system.
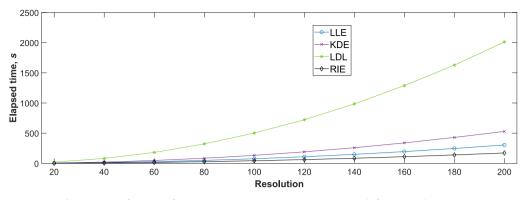
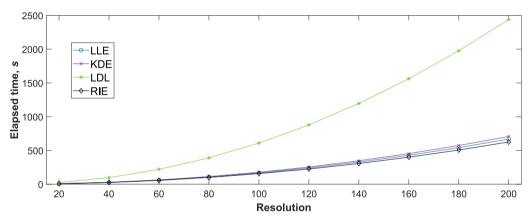**Fig. 13.** The performance of the parametric chaotic set construction methods for the Rossler system.

Fig. 14. The performance of the parametric chaotic set construction methods for the Newton-Leipnik system.

significantly decrease while the number of points in the recurrence plot increases (parameter T_{dec} in calculation algorithm, Appendix D).

Theoretical estimation of time complexity for RIE and LLE algorithms is $O(N)$ because they include one loop of N iterations. The LDL computation requires the construction of the recurrence plot, which estimates the distance between two points of the entire time series. Thus, the time complexity of this algorithm is $O(N^2)$ (Appendix D). The time complexity of the KDE method depends significantly on the number of local maxima X_p^j found using function *peaks*(·) (Appendix C). In the worst case, with a large value of X_p^j, the time complexity will be $O(N^2)$.

To experimentally compare the performance of the studied algorithms we plotted two sets of performance graphs. In the first set, as we already did in the previous experiment, we stepped the simulation time by $\Delta t = 50$ s and calculated the time costs of constructing the parametric chaotic set in 50×50 pixels. The results are presented in Figs. 10–12. The obtained graphs show that the actual computational costs of the compared algorithms are rather different from the theoretical ones. The complexity $O(N^2)$ is demonstrated only by the LDL algorithm. The curve for the KDE algorithm nearly corresponds to the linear law, since the number of local maxima is insignificant in comparison to the size of the time series.

The second step of the performance evaluation was to measure the time needed to construct the parametric chaotic set with desirable precision and resolution. We measured the elapsed time by changing the resolution for each dimension from 20 to 200 pixels (Figs. 13–15). One can see that the LDL calculation is the slowest way to construct the parametric set. To obtain 200×200 pixels two-parametric chaotic set it requires twice more time than other considered algorithms. The performance of the LLE algorithm is comparable to the KDE method in the cases of the Newton-Leipnik and Marioka-Shimizu systems. The proposed RIE algorithm appears to be the fastest among the compared methods. However, the performance can slightly depend on the simulated system.
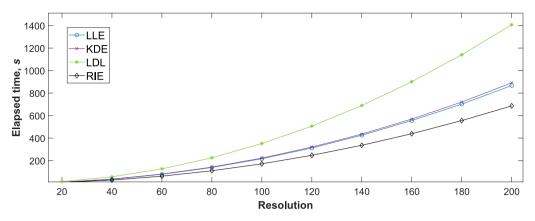
Fig. 15. The performance of the parametric chaotic set construction methods for the Marioka-Shimizu system.

5. Conclusion

The main target of this study was to introduce a novel technique for chaotic system analysis in comparison to various algorithms of parametric chaotic set construction. We proposed the new quantitative metrics based on the relative error of two numerical models obtained by semi-implicit numerical integration methods, and compared this technique with three common methods of dynamical analysis. The convergence time of the quantitative metrics was set using the technique based on the perceptual hash. Experiments have discovered that the proposed method of determining the minimum time for the chaotic system simulation is suitable for evaluating all of the considered metrics. Then, the performance of the investigated algorithms for parametric chaotic set construction was estimated. We explicitly show that the computational complexity of algorithms may differ from the theoretical assumptions due to parameter variation in the algorithms and the properties of the investigated system. Considering the Rossler, Newton-Leipnik and Marioka-Shimizu chaotic systems as examples, we established that the RIE method appears to be the fastest algorithm among studied techniques. In addition, the proposed algorithm does not require long-term simulation to obtain reliable results. Being compared with the traditional LLE evaluation method, the RIE algorithm treats the trajectories divergence that is caused by the difference in semi-implicit numerical integration methods with different commutation matrices, but of the same accuracy order, stability and number of arithmetical operations. Thus, there is no need for the procedure of choosing the initial divergence value or the normalization after a certain number of steps. The proposed metrics allows distinguishing the chaotic and periodic behavior as well as traditional analysis techniques. It should also be noted that RIE metrics is better-suited to the investigation of conservative chaotic systems being based on the geometric integration approach. Moreover, the extra degree of freedom typical for other techniques often leads to complicated tuning procedures. It not only affects the results of analysis but easily can confuse researchers when they use these algorithms thoughtlessly. Second, the most advanced feature of the proposed technique is low computational costs. All post-processing methods applicable to the other techniques can be applied to the RIE metrics as well. Finally, the application of several techniques is usually required to properly investigate the system. Therefore, we hope that RIE can become a part of this complex analysis software.

Studying systems with different types of dynamic behavior using considered techniques and further verification of obtained parametric chaotic sets will be the topic of our future research. Moreover, we are going to consider various approaches for reducing the time of constructing high-resolution parametric chaotic sets and techniques to improve the algorithms for calculating the quantitative metrics of chaotic systems. Particularly, it is necessary to thoroughly describe the technique of choosing the smoothing bandwidth in statistical methods of bifurcation analysis, as well as the optimal size of the neighborhood when constructing recurrence plots.

Funding

Declaration of Competing Interest

The authors declare that they have no known competing financial interests or personal relationships that could have appeared to influence the work reported in this paper.

CRediT authorship contribution statement

Denis N. Butusov: Writing - original draft, Project administration, Supervision, Methodology, Funding acquisition. **Dmitriy O. Pesterev:** Writing - review & editing, Data curation, Visualization, Software. **Aleksandra V. Tutueva:** Investigation, Writing - original draft, Software, Validation. **Dmitry I. Kaplun:** Resources, Writing - review & editing, Data curation. **Erivelton G. Nepomuceno:** Writing - review & editing, Methodology, Validation, Formal analysis.

Acknowledgement

Appendix A. List of used notations

Notation	Description
C_t	continuous operator of the system evolution on time t
h	integration step
F_h	discrete operator of the system evolution obtained by applying numerical integration method with integration step h
d	dimension of ODE system
t	continuous variable of time
t_n	discrete time
x^j	state variable of the system with index j
x_i^j	state variable of the system with index j in time t_i
$\mathbf{x} = (x^1, x^2, \ldots, x^d)$	vector of the system state variables
$\mathbf{x}_i = (x_i^1, x_i^2, \ldots, x_i^d)$	vector of the system state variables in time t_i
$X^j = (x_1^j, x_2^j, \ldots, x_N^j)$	time series of the state variable x^j of length N
T_s	simulation time
T_t	transient process time
T_n	normalization time
T_{dec}	decimation time
h_s	smoothing bandwidth of the kernel density estimation
k_s	sampling coefficient
δ	infinite small divergence between two initial conditions
ε	finite divergence between two initial conditions
ϵ	neighborhood distance of the recurrence plot
λ	largest Lyapunov exponent value
ρ	period of the ODE system solution
ν	inverse value of longest diagonal line length
ω	average logarithmic local truncation error
$\lVert \cdot \rVert$	Euclidean norm
$\widehat{\zeta}$	estimation of the ζ
$\sharp X$	cardinality of the set X

Appendix B. LLE calculation algorithm

---

input : a discrete operator of the system evolution F_h, a integration step h, an initial time t_0, an initial condition $\mathbf{x}_0$, a simulation time T_s, a normalization time T_n, an initial divergence ε

output: The largest Lyapunov exponent λ

$\lambda = 0$;

$t = t_0$;

$\mathbf{x} = \mathbf{x}_0$;

$\mathbf{y} = \mathbf{x}_0 + \varepsilon$;

for $i = 1 : T_s/T_n$ **do**

    for $j = 1 : T_n/h$ **do**

        Compute next iteration;

        $\mathbf{x} = F_h(\mathbf{x}, t)$;

        $\mathbf{y} = F_h(\mathbf{y}, t)$;

        $t = t + h$;

        Compute the rate of exponential divergence;

        $\lambda = \lambda + \ln \frac{||\mathbf{y}-\mathbf{x}||}{||\varepsilon||}$;

    end

    Normalize the distance;

    $\mathbf{y} = \mathbf{x} + \varepsilon \frac{\mathbf{y}-\mathbf{x}}{||\mathbf{y}-\mathbf{x}||}$;

end

Compute the average rate of exponential divergence;

$\lambda = \lambda/T_s$;

Appendix C. KDE calculation algorithm

---

input : A discrete operator of the system evolution F_h, an integration step h, an initial condition x_0, an initial time t_0, a simulation time T_s, a variable index j, a smoothing step h_s, a sampling coefficient k_s

output: Estimation of the ODEs solution period $\widehat{\rho}$

$N = T_s/h$;

Compute solution;

for $i = 0 : N - 1$ **do**

    $\mathbf{x}_{i+1} = F_h(\mathbf{x}_i, t_0 + ih)$;

end

Take the variable x_j time series;

$X^j = (x_0^j, x_1^j, \ldots, x_N^j)$;

Find the magnitude and the number of local maxima;

$X_p^j = peaks(X^j)$;

$N_p = \sharp X_p^j$;

Estimate PDF and apply discretization to it;

for $k = 0 : N_p k_s - 1$ **do**

    $y_k = \min(X_p^j) + k\frac{\max(X_p^j)-\min(X_p^j)}{N_p k_s - 1}$;

    $z_k = \frac{1}{N_p h_s} \sum_{i=1}^{N_p} \exp\left(-\frac{(y_k - x_i^j)^2}{2h_s^2}\right)$;

end

$Z^j = (z_0, z_1, \ldots, z_{N_p k_s - 1})$;

Count local maxima in PDF discretization;

$\widehat{\rho} = \sharp peaks(Z^j)$;

Appendix D. LDL calculation algorithm

---

input : A discrete operator of the system evolution F_h, a integration step h, an initial condition $\mathbf{x}_0$, an initial time t_0, a simulation time T_s, a decimation time T_{dec}, a neighborhood distance ϵ

output: A inverse value of the longest diagonal line ν

DL $= -1$;

LDL $= 0$;

$t = t_0$;

$\mathbf{x} = \mathbf{x}_0$;

for $i = 1 : T_s/T_{dec}$ **do**

    for $j = 1 : T_{dec}/h$ **do**

        Compute next iteration;

        $\mathbf{x} = F_h(\mathbf{x}, t)$;

        $t = t + h$;

    end

    $\mathbf{x}_i = \mathbf{x}$;

end

Find LDL;

for $i = 1 : T_s/T_{dec} - 1$ **do**

    for $j = 0 : T_s/T_{dec} - i$ **do**

        if $||\mathbf{x}_{j+i} - \mathbf{x}_j|| < \epsilon$ **then**

            DL $=$ DL $+ 1$;

        else

            DL $= -1$;

        end

    end

    LDL $= \max(\text{LDL}, \text{DL})$;

end

$\nu = 1/\text{LDL}$;

References

[1] Kemih K, Ghanes M, Remmouche R, Senouci A. A novel 5D-dimensional hyperchaotic system and its circuit simulation by EWB. Math Sci Lett 2015;4(1):1–4.

[2] Petrzela J, Gotthans T. New chaotic dynamical system with a conic-shaped equilibrium located on the plane structure. Appl Sci 2017;7(10):976.

[3] Elhadj Z, Sprott JC. Simplest 3D continuous-time quadratic systems as candidates for generating multiscroll chaotic attractors. Int J Bifurc Chaos 2013;23(07):1350120.

[4] Rajagopal K, Akgul A, Moroz IM, Wei Z, Jafari S, Hussain I. A simple chaotic system with topologically different attractors. IEEE Access 2019;7:89936–47.

[5] Lu H, Niu R, Liu J, Zhu Z. A chaotic non-dominated sorting genetic algorithm for the multi-objective automatic test task scheduling problem. Appl Soft Comput 2013;13(5):2790–802.

[6] Dudul SV. Prediction of a lorenz chaotic attractor using two-layer perceptron neural network. Appl Soft Comput 2005;5(4):333–55.

[7] Sprott JC. A proposed standard for the publication of new chaotic systems. Int J Bifurc Chaos 2011;21(09):2391–4.

[8] Leonov GA, Kuznetsov NV. Hidden attractors in dynamical systems. from hidden oscillations in Hilbert–Kolmogorov, Aizerman, and Kalman problems to hidden chaotic attractor in chua circuits. Int J Bifurc Chaos 2013;23(01):1330002.

[9] Avrutin V, Schanz M, Banerjee S. Multi-parametric bifurcations in a piecewise–linear discontinuous map. Nonlinearity 2006;19(8):1875.

[10] Abrams DM, Strogatz SH. Chimera states in a ring of nonlocally coupled oscillators. Int J of Bifurc Chaos 2006;16(01):21–37.

[11] Zgurovsky MZ, Kasyanov PO. Qualitative and quantitative analysis of nonlinear systems. Springer; 2018.

[12] Alpar O. A new chaotic map with three isolated chaotic regions. Nonlinear Dyn 2017;87(2):903–12.

[13] Zhang W, Wang J. Nonlinear stochastic exclusion financial dynamics modeling and complexity behaviors. Nonlinear Dyn 2017;88(2):921–35.

[14] Ausloos M. Measuring complexity with multifractals in texts. translation effects. Chaos Solitons Fract 2012;45(11):1349–57.

[15] Shuang Z, Yong F, Wen-Yuan W. A novel method to identify the scaling region of correlation dimension. Acta Phys Sin 2015;64(13).

[16] Kuznetsov N, Mokaev T. Numerical analysis of dynamical systems: unstable periodic orbits, hidden transient chaotic sets, hidden attractors, and finite–time Lyapunov dimension. J Phys 2019;1205(1):012034.

[17] Panchuk A, Sushko I, Schenke B, Avrutin V. Bifurcation structures in a bimodal piecewise linear map: regular dynamics. Int J Bifurc Chaos 2013;23(12):1330040.

[18] Nepomuceno EG, Junior HMR, Martins SA, Perc M, Slavinec M. Interval computing periodic orbits of maps using a piecewise approach. App Math Comput 2018;336:67–75.

[19] Trauth MH, Asrat A, Duesing W, Foerster V, Kraemer KH, Marwan N, et al. Classifying past climate change in the Chew Bahir basin, southern Ethiopia, using recurrence quantification analysis. Clim Dyn 2019:1–16.

[20] Sanjuán MA. Using nonharmonic forcing to switch the periodicity in nonlinear systems. Phys Rev E 1998;58(4):4377.

[21] Nepomuceno EG, Mendes EM. On the analysis of pseudo-orbits of continuous chaotic nonlinear systems simulated using discretization schemes in a digital computer. Chaos Solitons Fract 2017;95:21–32.

[22] Butusov D, Karimov A, Tutueva A, Kaplun D, Nepomuceno EG. The effects of Padé numerical integration in simulation of conservative chaotic systems. Entropy 2019;21(4):362.

[23] Teixeira J, Reynolds CA, Judd K. Time step sensitivity of nonlinear atmospheric models: numerical convergence, truncation error growth, and ensemble design. J Atmos Sci 2007;64(1):175–89.
[24] Butusov DN, Ostrovskii VY, Pesterev DO. Numerical analysis of memristor-based circuits with semi-implicit methods. In: 2017 IEEE conference of Russian young researchers in electrical and electronic engineering (EIConRus). IEEE; 2017. p. 271–6.
[25] Karimov AI, Butusov DN, Tutueva AV. Adaptive explicit-implicit switching solver for stiff ODEs. In: 2017 IEEE conference of Russian young researchers in electrical and electronic engineering (EIConRus). IEEE; 2017. p. 440–4.
[26] Butusov DN, Ostrovskii VY, Tutueva AV, Savelev AO. Comparing the algorithms of multiparametric bifurcation analysis. In: 2017 XX IEEE international conference on soft computing and measurements (SCM). IEEE; 2017. p. 194–8.
[27] Lyapunov AM. The general problem of motion stability. Ann Math Stud 1892;17.
[28] Shimada I, Nagashima T. A numerical approach to ergodic problem of dissipative dynamical systems. Prog Theor Phys 1979;61(6):1605–16.
[29] Wolf A, Swift JB, Swinney HL, Vastano JA. Determining Lyapunov exponents from a time series. Physica D 1985;16(3):285–317.
[30] Marwan N, Romano MC, Thiel M, Kurths J. Recurrence plots for the analysis of complex systems. Phys Rep 2007;438(5–6):237–329.
[31] Eckmann J, Kamphorst SO, Ruelle D, et al. Recurrence plots of dynamical systems. World Sci Ser Nonlinear Sci SerA 1995;16:441–6.
[32] Butusov D, Tutueva A, Homitskaya E. Extrapolation Semi-implicit ODE solvers with adaptive timestep. In: 2016 XIX IEEE international conference on soft computing and measurements (SCM). IEEE; 2016. p. 137–40.
[33] Theiler J, Smith LA. Anomalous convergence of Lyapunov exponent estimates. Phys Rev E 1995;51(4):3738.
[34] Monga V, Evans BL. Perceptual image hashing via feature points: performance evaluation and tradeoffs. IEEE Trans Image Proces 2006;15(11):3452–65.
[35] Hénon M. A two-dimensional mapping with a strange attractor. In: The theory of chaotic attractors. Springer; 1976. p. 94–102.
[36] Zaslavsky G. The simplest case of a strange attractor. Phys Lett A 1978;69(3):145–7.
[37] Chirikov BV. Research concerning the theory of non-linear resonance and stochasticity. Tech. Rep.. CM-P00100691; 1971.
[38] Lorenz EN. Deterministic nonperiodic flow. J Atmos Sci 1963;20(2):130–41.
[39] Rössler OE. An equation for continuous chaos. Phys Lett A 1976;57(5):397–8.
[40] Sprott JC. Some simple chaotic flows. Phys Rev E 1994;50(2):R647.
[41] Moore D, Toomre J, Knobloch E, Weiss N. Period doubling and chaos in partial differential equations for thermosolutal convection. Nature 1983;303(5919):663.
[42] Gang H, Kaifen H. Controlling chaos in systems described by partial differential equations. Phys Rev Lett 1993;71(23):3794.
[43] Linh VH, Mehrmann V. Lyapunov, Bohl and Sacker-Sell spectral intervals for differential-algebraic equations. J Dyn Differ Equ 2009;21(1):153–94.
[44] Leipnik R, Newton T. Double strange attractors in rigid body motion with linear feedback control. Phys Lett A 1981;86(2):63–7.
[45] Newton TA, Martin D, Leipnik R. A double strange attractor. In: Dynamical systems approaches to nonlinear problems in systems and circuits. Philadelphia: SIAM; 1988. p. 117–27.
[46] Shimizu T, Morioka N. On the bifurcation of a symmetric limit cycle to an asymmetric one in a simple model. Phys Lett A 1980;76(3–4):201–4.
[47] Kahan W. IEEE standard 754 for binary floating-point arithmetic. Lect Notes Status IEEE 1996;754(94720–1776):11.